Response to Reviewer #2 Comments

General Comments

General Comment 1

This work describes laboratory studies to comprehensively characterize gases and particles in fresh and aged peat biomass burning organic aerosol (BBOA). A Potential Aerosol Mass Oxidation Flow Reactor (PAM-OFR) was used to oxidize peat emissions. Filter-based measurements provided $PM_{2.5}$ mass concentrations, elemental concentrations, eight different thermally-resolved carbon fractions (OC, EC, pyrolyzed carbon), organic acids, water soluble organic carbon, carbohydrate concentrations, NH_4, and HNO_3 concentrations. Mass reconstruction and moisture content analyses are also provided. This manuscript addresses a lack of peat BBOA related source profiles, providing a wealth of information on gas- and particle-phase peat BBOA chemical composition with and without atmospheric aging. The intercomparison between peat samples from six locations to represent different biomes is particularly novel.

Although this work has the potential to be highly useful for future source apportionment studies, I do not recommend publication unless major revisions are made. In particular, there is very little information provided on PAM-OFR operation characteristics, which makes it extremely difficult to assess whether the reactor was used properly to mimic atmospherically relevant conditions. In reading this paper, it seems as though there have been two additional manuscripts submitted using this data set and/or these techniques (Watson et al., 2019, and Cao et al., 2019), and although they are repeatedly cited, they have not yet been peer reviewed/published (per the citations), so I was unable to verify if the necessary information has been provided in these works. This significantly weakens the impact of this work, since the techniques are neither verifiable nor repeatable. Specific suggestions for improvement are provided in the following general and technical/minor comments. BBOA oxidation is incredibly challenging to characterize using a PAM-OFR due to chemical and physical heterogeneity and rapid/complex kinetics. More attention should therefore be given to contextualizing the results presented here in light of PAM-OFR challenges. The PAM wiki is a useful site that provides recommendations for reactor operation (https://sites.google.com/site/pamwiki/hardware/tutorial_and_recs).

Response 1 (Including Parts A, B, and C)

- **Part A:** The following has been added to the Section S.1 (Experimental Details and Oxidation Flow Reactor Operation [pages S-2 to S4]) supplemental material to document the OFR approach. Excerpts are taken from this to address the subsequent comments.

Oxidation Flow Reactors (OFRs) intend to simulate photochemical changes in gas and particle mixtures as they age during atmospheric transport. This is accomplished by directing fresh emissions through a chamber that is illuminated with ultraviolent (UV) light to simulate the Sun's illumination of the mixture. OFRs differ from smog chambers in that the UV radiation is more intense and there is a continuous flow through the system, rather than the stagnant mixture that is examined in the smog chamber at UV levels closer to ambient levels (Hidy, 2019; Lee et al., 2009). Various OFR systems have been developed and applied (Aerodyne, 2019b; Bin Babar et al., 2017; Cazorla and Brune, 2010; Ezell et al., 2010; Huang et al., 2017; Karjalainen et al., 2016; Lambe et al., 2011; Mitroo et al., 2018; Pourkhesalian et al., 2015; Reece et al., 2017; Smith et al., 2009) since the original Teflon bag of Kang et al. (2007) that was externally illuminated with mercury vapor lamps. These units range in volume from 0.15 L (Keller and Burtscher, 2012) to 1200 L (Ezell et al., 2010) and are made from fluorinated ethylene propylene (FEP) Teflon films, stainless steel, quartz or Iridite/Anodine coated aluminum with the intent to

minimize reactions with the chamber walls. Although many published articles reference the characterization and operational details of Kang et al. (2007), it is evident that there have been many changes since their initial development.

Important OFR design parameters are (Huang et al., 2017): 1) gas introduction mixing prior to and within the OFR chamber; 2) chamber volume and range of flow rates that determine residence time within the chamber; 3) reaction chamber materials that minimize artifacts (e.g., reactant adsorption and outgassing); and 4) sensors applied to detect the types of reactants and end-products. General findings are: 1) larger diameters and shorter residence times minimize gas and particle losses to chamber surfaces; 2) rapid mixing of pollutants provides more accurate reaction rate measurements; and 3) passivated conductive surfaces minimize electrostatic effects on particles. Although the Caltech Photooxidation Flow Tube reactor (Huang et al., 2017) appears to be the best characterized via modeling and experiment, the Aerodyne (2019b) potential aerosol mass (PAM)-OFR is in more widespread use owing to its compactness, reliability, expanding user-base (PAMWiki, 2019), and commercial availability. The Aerodyne OFR was used for the experiments reported here.

Figure S1 illustrates the configuration for these experiments. Two tubular low-pressure mercury (Hg) lamps in the OFR with Teflon sleeves provided UV light at 185 and 254 nm wavelengths (BHK, 2019) and two lamps with doped quartz sleeves provided illumination at 254 nm. Lamps were cooled by a continuous flow of relatively inert, nitrogen (N_2) gas. The main reactions for this OFR185 mode that create O_3, OH (hydroxyl radical), and HO_2 (hydroperoxyl radical) oxidants are:

$$H_2O + h\nu\ (185\ nm) \rightarrow OH + H \quad (1)$$

$$O_2 + h\nu\ (185\ nm) \rightarrow 2O(^3P) \quad (2)$$

$$O_2 + O(^3P) \rightarrow O_3 \quad (3)$$

$$O_3 + h\nu\ (254\ nm) \rightarrow O_2 + O(^1D) \quad (4)$$

$$O(^1D) + H_2O \rightarrow 2OH \quad (5)$$

$$H + O_2 \rightarrow HO_2 \quad (6)$$

The OH is most influential in photochemical aging, and OH production within the OFR is related to the Hg lamp intensity, which in turn is related to the voltages applied to the lamps. Bhattarai et al. (2018) demonstrate that UV fluxes are almost linearly associated with lamp voltage from 2 to 7 V, and similar linear results were found for the profile aging tests reported here (Cao et al., 2019). OH production is related to lamp intensity by inference from first order reactions of OH with SO_2 which has a well-characterized rate constant ($k_{SO2,OH}$= 9.49x10^{-13} cm^3 molecule^{-1} sec^{-1} at 1 atm and 298 °K) (Davis et al., 1979; Sander et al., 2006) by the relationship:

$$OH = -1/k_{SO2,OH}\ \ln (C_{SO2,out}/C_{SO2,in}) \quad (7)$$

where

$k_{SO2,OH}$= *reaction rate of SO_2 with OH (cm^3 molecule^{-1} sec^{-1})*
$C_{SO2,in}$=*SO_2 concentration injected into the OFR (ppb)*
$C_{SO2,out}$=*SO_2 concentration at the OFR outlet (ppb)*

UV lamps were operated at 2 and 3.5 volts with a flow rate of 10 L min^{-1} and a plug-flow residence time of ~80 s in the 13.3 L anodine-coated reactor, which translates to OH exposures (OH_{exp}) of ~2.6 x 10^{11} and 8.8 x 10^{11} molecules-sec cm^{-3} at 2 volts and 3.5 volts, respectively. These values for OH_{exp} are within the range of 1x10^{10} to ~2x10^{12} molecules-sec cm^{-3} reported in

other OFR experiments. The lamps were powered and brought into steady state operations before drawing the sample stream through the OFR

The Aerodyne OFR surface-to-volume ratio is 0.24 cm^{-1}, which is larger than many of the other OFR types and is intended to minimize particle and gas losses with lamp off. SO_2 concentrations measured ranging from 100 to 800 ppb at the OFR inlet showed less than 1% changes when measured at the OFR outlet. Similar results were found for carbon monoxide (CO) and ozone (O_3), indicating minimal losses to the reactor surfaces. This is in contrast to the Teflon bag of Kang et al. (2007) that experienced SO_2 losses as high as 20%. Lambe et al.(2011) found transmission efficiencies of 0.91±0.09 for CO_2 and 1.2±0.4 for SO_2 with a later quartz glass OFR design.

Lambe et al. (2011) found particle transmission efficiencies exceeding 80% for mobility diameters >150 nm, but as low as 40% for 50 nm particles with a quartz OFR. Karjalainen et al. (2016) measured 60% particle losses for ~20 nm particles, ~25% particle losses for 50 nm particles, and <10% losses for particle sizes >100 nm with a stainless steel OFR. Palm et al. (2016) compared mass concentrations in ambient air within a forest with the same air drawn through an Aerodyne OFR and transfer lines, finding only a 4% particle loss. Bhattarai et al. (2018) found similar results for ammonium sulfate ($(NH_4)_2SO_4$) particles, with 50% transmission for 20 nm particles and >90% transmission for particles >100 nm.

For this study, UV lamp stability and linearity was determined by moving a TOCON_C6 photodiode (Sglux GmbH, Germany) detector along the central axis of the OFR and recording its readings as function of the voltage supplied to the lamps, verifying that the UV flux was linearly associated with lamp voltage from 2 to 7 V, but it was undetectable for UV <1.5V and leveled off at ~350 $\mu W\ cm^{-2}$ in the range of 7-10 V. Experiments were limited to 2 and 3.5 V which is well-within the linear range. Irradiation fluxes were 2.5 x 10^{13} photons $cm^{-2}\ s^{-1}$at 2 V and 12.5 x 10^{13} photons $cm^{-2}\ s^{-1}$ at 3.5 V. Fluxes were constant both in time and along the OFR axis, indicating that consistent oxidant amounts can be produced for a given voltage within the linear range, similar to the findings of Bhattarai et al. (2018). Periodic performance tests of light intensity should be made over time as there may be some deterioration of lamp performance with use, and the measurements need to be repeated when lamps are replaced.

Since high O_3 concentrations were generated when UV lamps were on, a potassium iodide (KI) denuder (1/3 KI with 2/3 silica) was installed at the outlet of the reactor to remove over 99.99% of the O_3 and maintain a stable baseline of < 20 ppb. This possibly compromised some of the potassium ion measurement in the aged profiles.

As discussed in the main text, the biggest uncertainty is not the estimation of oxidant exposure in the OFR, but the conversion of this exposure to atmospheric aging times. Changes in the atmospheric multipollutant environment as emissions from several sources mix in the atmosphere are not represented within the OFR. Added to this are the unknown effects of the high oxidant exposures within the OFR relative to atmospheric exposures and the wide variability of atmospheric OH from the assumed 1.5x10^6 molecules cm^{-3} which is commonly, but not universally, used to translate OH exposure to atmospheric aging.

- **Part B:** While the Reviewer approaches this from the perspective of an OFR expert, our results are more directed toward the receptor-oriented source apportionment community. The OFR portion of the experiment is not the controlling uncertainty in terms of source profiles. We do not maintain that our results or our approach are the only ways to account

for profile aging, but they do fill a needed knowledge gap. To this end we add the following context (Lines 90-110) in the "Introduction" section:

Despite this lack of peat-specific fresh and aged source profiles, results have been published for source apportionment in Indonesia (See et al., 2007), Malaysia (Fujii et al., 2017), Singapore (Budisulistiorini et al., 2018), and Ireland (Dall'Osto et al., 2013; Kourtchev et al., 2011; Lin et al., 2019). These have involved sampling under near-source and far from-source dominated environments, such as the 2015 Indonesia burning episode to determine changes in thermally-derived carbon fractions with aging (Tham et al., 2019), and inference of aged peat-burning profiles from positive matrix factorization (PMF) application to chemically-speciated ambient PM samples (Fujii et al., 2017). Budisulistiorini et al. (2018) observe that "…atmospheric processing of aerosol particles in haze from Indonesian wildfires has scarcely been investigated. This lack of study inhibits a detailed treatment of atmospheric processes in the models, including aerosol aging and secondary aerosol formation."

Changes in source profiles have been demonstrated in large smog chambers (Pratap et al., 2019), wherein gas/particle mixtures are illuminated with ultraviolet (UV) light for several hours and their end products are measured. Such chambers are specially constructed and limited to laboratory testing. A more recent method for simulating such aging is the oxidation flow reactor (OFR), based on the early studies of Kang et al. (2007), revised and improved by several researchers (e.g., Jimenez, 2018; Lambe et al., 2011), and commercially available from Aerodyne (2019a, b). Although the Aerodyne potential aerosol mass (PAM)-OFR has many limitations, as explained in the supplemental material (Section S.1), it is a practical method for understanding how profiles might change with different degrees of atmospheric aging. A growing users group (PAMWiki, 2019) provides increasing knowledge of its characteristics and operations.

- **Part C:** The experimental section in the main text has been modified as follows to qualify the intermediate- and well-aged profiles (Lines 124–157):

The supplemental material describes sampling configuration shown in Fig. S1 and OFR operation. Briefly, peat smoke generated in a laboratory combustion chamber (Tian et al., 2015) was diluted with clean air (by factors of three to five) to allow for nucleation and condensation at ambient temperatures (Watson et al., 2012). These diluted emissions were then passed through an unmodified Aerodyne PAM-OFR in the OFR185 mode without ozone (O_3) injection. Hydroxyl radical (OH) production as a function of UV lamp voltage was estimated by inference from sulfur dioxide (SO_2) decay using well-established rate constants. UV lamps were operated at 2 and 3.5 volts with a flow rate of 10 L min^{-1} and a plug-flow residence time of ~80 s in the 13.3 L anodine-coated reactor, which translates to OH exposures (OH_{exp}) of ~2.6 x 10^{11} and ~8.8 x 10^{11} molecules-sec cm^{-3} at 2 volts and 3.5 volts, respectively.

Transport times between source and receptor of 1 to 10 days are typical of peat burning plumes, and the two OH_{exp} estimates were selected to examine intermediate (~2 days) and long-term (~7 days) atmospheric aging. Other emissions aging experiments (e.g., Bhattarai et al., 2018) cite Mao et al. (2009) for a 24-hour average atmospheric OH concentration (OH_{atm}) of 1.5x10^6 molecules cm^{-3}. This number appears nowhere in the text of Mao et al. (2009), but it corresponds to the ground-level median value in Mao's Figure 8 plot of OH vs. altitude for Asian outflows over the Pacific Ocean. The individual measurements in the plot range from OH_{atm} near-zero to 5.3x10^6 molecules cm^{-3}. Altshuller (1989) concluded that "The literature contains reports of atmospheric OH radical concentrations measured during daylight hours ranging from 10^5 molecule cm^{-3} to over 10^8 molecule cm^{-3}, but almost all of the values reported are below 5x10^7 molecules cm^{-3}."

Stone et al. (2012) report atmospheric values ranging from $1.1x10^5$ molecules cm^{-3} in polar environments to $1.5x10^7$ molecules cm^{-3} in a vegetated forest. Uncertainties in OH_{exp} within the OFR are, therefore, not the controlling uncertainty in estimating profile aging times. Added to this uncertainty are reactions among emission constituents that are not embodied in the OFR185 mode that tend to suppress OH_{exp} with respect to that estimated by the SO_2 calibration (Li et al., 2015; Peng et al., 2015; Peng et al., 2016; Peng and Jimenez, 2017; Peng et al., 2018). The "OFR Exposure Estimator" available from the PAMWiki (2019) intends to estimate this OH_{exp}, but detailed VOC from these experiments are insufficient to apply it. The nominal 2- and 7-day aging times determined by dividing OH_{exp} by Mao's $1.5x10^6$ molecules cm^{-3} are subject to these uncertainties, which may increase or decrease the aging time estimates. However, these uncertainties, along with other uncertainties related to peat sample selection, moisture content, and laboratory burning conditions do not negate the value of the measurements reported here. There are distinct differences in the fresh, intermediate-aged, and well-aged profiles that address the concerns expressed by Budisulistiorini et al. (2018)..

General Comment 2

In general, there is a lack of information provided regarding PAM-OFR operating conditions. What were the flow rates (and by extension residence times) through the PAM-OFR? What were dilution ratios? Were dilution ratios kept constant for samples collected before and after the PAM-OFR? Was the reactor allowed to reach steady state prior to sample collection? What were typical photon fluxes measured at each oxidation condition? Without this information, the results are entirely without context and essentially meaningless.

Response 2

As noted in the above revisions, the air stream extracted from the burn chamber was diluted with clean air by factors of 3 to 5, flow rate through the OFR was 10 L min^{-1}, which corresponded to an 80 s plug flow aging time, and the UV lamps were warmed up to steady state prior to each burn. Photon fluxes are also specified in the revisions.

General Comment 3

How was the OFR calibrated for these studies (e.g., with SO2? CO? With or without BBOA?)? It seems that this is not the only manuscript to come out of this data set – is the PAM-OFR calibration procedure discussed in related articles? However, it would be good to provide even a basic description of calibration details here, perhaps in the supplement.

Response 3

As noted in the above revisions to the supplemental material, OH concentrations were estimated from SO_2 decay following the procedures recommended by past studies and using known reaction constants..

General Comment 4

Was external OH reactivity ($OHRext \sim \Sigma k_i c_i$, where k_i is the OH reaction rate constant for species i and c_i is the concentration of reacting species i) characterized in this or other studies? Peng et al. (2015, 2016) and Li et al. (2015) describe suppression of OH by interfering VOC species. The OHRext should be characterized/estimated for your system, particularly because many different VOCs generated from biomass burning can react externally with OH. It should be explicitly stated whether or not parallel gas-phase measurements (e.g., from a PTR-MS) were conducted. If so, the authors should provide some analysis and discussion about how the measured

VOCs potentially interfered with their OHRext. If not, hopefully the authors attempted to remove VOCs (e.g., with VOC denuders), or, failing to at least do that, provide some discussion about the potential for interference. Without any attention to this caveat of OFR experiments, the results are questionable.

Response 4

Potential OH_{exp} is recognized in revisions to the experimental section of the main text, and it is noted that the detailed VOC data needed for this was not available for these experiments. A case is made that this is not the controlling uncertainty for converting OH exposure to aging times, as the $1.5x10^6$ molecules cm^{-3} atmospheric concentration is unjustifiably assumed by many articles that translate OH_{exp} to days of aging. Whether the aging is 1 to 3 days for nearby pollution sources or 5 to 8 days for distant regional sources doesn't matter for source apportionment purposes at our current understanding of profile aging. The large differences between fresh, intermediate-aged, and well-aged profiles is readily apparent from the comparisons.

General Comment 5

With OFR-185, photolysis at both 254 nm and 185 nm may occur, particularly at high light intensities. Peng et al. (2016) provides a detailed examination of exposure ratios (photon flux/OHexp) that have improved understanding of the potential for photolysis for different species. I recommend examining this manuscript (particularly figures 1 and 2) and discussing the potential for photolysis under your experimental conditions. The calculation for percent interference by photolysis is straightforward and should be performed for any OFR study.

Response 5

With due respect for the Reviewer's OFR expertise, we refer to Response 4. This is not a study of the OFR, but of potential source profile changes.

General Comment 6

With OFR-185, HOx recycling can impact OH formation (Peng et al., 2015, Palm et al., 2016). As with OHRext and photolysis, the impact of HOx recycling (the removal of OH through $H2O + h\upsilon\ (185nm) \rightarrow H + OH$, then $H + O2 \rightarrow HO2$) under the experimental conditions needs to be addressed.

Response 6

With due respect for the Reviewer's OFR expertise, we refer to Response 4. This is not a study of the OFR, but of potential source profile changes. This would only affect the assumed aging times, for which we have demonstrated that the controlling uncertainty derives from the large variability in ambient OH exposures.

General Comment 7

In lines 238-240, differences in the sum of species at different levels of aging are attributed to semivolatile organic compound (SVOC) losses. Did you perform "dark" experiments (i.e., collect particles and gases through the PAM-OFR without the lights on) at any point? Particles and gases collected through the PAM might be subject to different losses compared to those collected before the PAM (Palm et al., 2016). Since you are comparing fresh and aged profiles, which were collected before and after the PAM, respectively, the potential for wall losses needs to be addressed.

Response 7

The above revisions describe experiments with CO, SO_2, and O_3 transmission through the reactor without UV radiation indicating negligible losses for these gases compared with earlier tests for Teflon and quartz surfaces. Apparently the passivated coating is effective. Tests by others are cited that show minimal particle losses.

General Comment 8

Several estimation equations have been developed to better characterize the PAM-OFR under different operating conditions. The OFR exposures estimator (available for download at https://sites.google.com/site/pamwiki/hardware/estimation-equations) is immensely helpful for understanding how different species are expected to interfere with desired OFR chemistry. Estimation equations for LVOC condensational losses for the PAM-OFR are also available on the PAM wiki. I would suggest using these tools to better characterize PAM-OFR operating conditions and citing the sources provided therein.

Response 8

With due respect for the Reviewer's OFR expertise, we refer to Response 4. This is not a study of the OFR, but of potential source profile changes. This would only affect the assumed aging times, for which we have demonstrated that the controlling uncertainty derives from the large variability in ambient OH exposures.

General Comment 9

In many places, more discussion of previous work is needed. In paragraph 2 of the introduction (lines 71-81), chemical profile measurements are discussed in the context of different fresh source contributions, yet the only citation provided is Chow et al. (2002). Please provide similar citations for each of these source contributions.

Response 9

The paragraph is revised as follows (Lines 63–77):

Many of these source profiles are compiled in country-specific source profile data bases (Cao, 2018; CARB, 2019; Liu et al., 2017b; Mo et al., 2016; Pernigotti et al., 2016; U.S.EPA, 2019) and have been widely used for source apportionment and speciated emission inventories.

Chemical profiles measured at the source have been sufficient to identify and quantify nearby, and reasonably fresh, source contributions. These source types include gasoline- and diesel-engine exhaust, biomass burning, cooking, industrial processes, and fugitive dust. Ambient VOC and PM concentrations have been reduced as a result of control measures applied to these sources, and additional reductions have been implemented for toxic materials such as lead, nickel, vanadium, arsenic, diesel particulate matter, and several organic compounds. As these fresh emission contributions in neighborhood- and urban-scale environments (Chow et al., 2002) decrease, regional-scale contributions that may have aged for intermediate (~2 days) or long (~7 days) periods prior to arrival at a receptor gain in importance. These profiles experience augmentation and depletion of chemical abundances owing to photochemical reactions among their gases and particles, as well as interactions upon mixing with other source emissions.

General Comment 10

As stated above, using a PAM-OFR to study BBOA is particularly challenging. There have been several studies that have improved the community's understanding of PAMOFR BBOA oxidation. This manuscript would greatly benefit from further discussion of previous BBOA PAM-OFR experiments to provide further context for results. A few that come to mind include Cubison

et al. (2011) and Ortega et al. (2013). Furthermore, to my knowledge, Sumlin et al. (2017) were the first to use an Aerodyne PAM-OFR to characterize both chemical and optical properties for aged and fresh peat BBOA. Given the similarity in fuel type, oxidation method, and scope of measurements, this study would provide useful context for your results in this and future publications (particularly the publication wherein UV/Vis and FTIR measurements will be discussed).

Response 10

The focus of this manuscript is on peat burning, not on all biomass burning. The manuscript is not intended to be a review of all work using OFRs, although this would be a useful contribution. The companion manuscript of Cao et al. (2019), which has unfortunately been under review for over three months, elaborated on this. A table (Table A) from that manuscript summarizing OFR uses for emissions testing is attached.

General Comment 11

In line 121, it is more appropriate to cite the first description of the PAM (Kang et al., 2007) and at least the Aerodyne PAM documentation (reference 2 in this manuscript, lines 524-525) rather than your own co-authored publications, unless the PAM-OFR was modified for this study in ways described in Cao et al. (2019). I was able to verify that Watson et al. (2019; published as a discussion paper in ACPD) does not describe any PAM-OFR modifications at this point, and therefore the citations are incomplete. If Cao et al. (2019) describes modifications to the PAM-OFR, this needs to be explicitly stated.

Response 11

Changes are made in both the Introduction (Lines 101–110) and Experiment (Lines 124-133) sections:

Lines 101-110:

Changes in source profiles have been demonstrated in large smog chambers (Pratap et al., 2019), wherein gas/particle mixtures are illuminated with ultraviolet (UV) light for several hours and their end products are measured. Such chambers are specially constructed and limited to laboratory testing. A more recent method for simulating such aging is the oxidation flow reactor (OFR), based on the early studies of Kang et al. (2007), revised and improved by several researchers (e.g., Jimenez, 2018; Lambe et al., 2011), and commercially available from Aerodyne (2019a, b). Although the Aerodyne potential aerosol mass (PAM)-OFR has many limitations, as explained in the supplemental material (Section S.1), it is a practical method for understanding how profiles might change with different degrees of atmospheric aging. A growing users group (PAMWiki, 2019) provides increasing knowledge of its characteristics and operations.

Lines 124-133:

The supplemental material describes sampling configuration shown in Fig. S1 and OFR operation. Briefly, peat smoke generated in a laboratory combustion chamber (Tian et al., 2015) was diluted with clean air (by factors of three to five) to allow for nucleation and condensation at ambient temperatures (Watson et al., 2012). These diluted emissions were then passed through an unmodified Aerodyne PAM-OFR in the OFR185 mode without ozone (O_3) injection. Hydroxyl radical (OH) production as a function of UV lamp voltage was estimated by inference from sulfur dioxide (SO_2) decay using well-established rate constants. UV lamps were operated at 2 and 3.5 volts with a flow rate of 10 L min^{-1} and a plug-flow residence time of ~80 s in the

13.3 L anodine-coated reactor, which translates to OH exposures (OH_{exp}) of ~2.6 x 10^{11} and ~8.8 x 10^{11} molecules-sec cm^{-3} at 2 volts and 3.5 volts, respectively.

Technical/Minor Comments:

1. Line 38: Either change "reconfirms" to "confirming," or change "reconfirms" to "confirms" and remove the preceding comma.

   Response: This paragraph in Abstract has been revised as follows (Lines 32-37):

   Organic carbon (OC) accounted for 58–85 % of $PM_{2.5}$ mass in fresh profiles with low EC abundances (0.67–4.4 %). OC abundances decreased by 20–33 % for well-aged profiles, with reductions of 3–14 % for the volatile OC fractions (e.g., OC1 and OC2, thermally evolved at 140 and 280 °C). Ratios of organic matter (OM) to OC abundances increased by 12–19 % from intermediate- to well-aged smoke. Ammonia (NH_3) to $PM_{2.5}$ ratios decreased after intermediate aging.

2. Lines 38-41: the use of "intermediate profile" in this sentence is confusing. Consider rewording this sentence for clarity.

   Response: The aging time is discussed in the first two paragraphs of the Abstract as shown in the following revised sentences (Lines 25-37):

   Smoke from laboratory chamber burning of peat fuels from Russia, Siberia, U.S.A. (Alaska and Florida), and Malaysia representing boreal, temperate, subtropical, and tropical regions was sampled before and after passing through a potential aerosol mass-oxidation flow reactor (PAM-OFR) to simulate intermediate-aged (~2 days) and well-aged (~7 days) source profiles. Species abundances in $PM_{2.5}$ between aged and fresh profiles varied by several orders of magnitude with two distinguishable clusters, centered around 0.1% for reactive and ionic species and centered around 10 % for carbon.

   Organic carbon (OC) accounted for 58–85 % of $PM_{2.5}$ mass in fresh profiles with low EC abundances (0.67–4.4 %). OC abundances decreased by 20–33 % for well-aged profiles, with reductions of 3–14 % for the volatile OC fractions (e.g., OC1 and OC2, thermally evolved at 140 and 280 °C). Ratios of organic matter (OM) to OC abundances increased by 12–19 % from intermediate- to well-aged smoke. Ammonia (NH_3) to $PM_{2.5}$ ratios decreased after intermediate aging.

3. Line 86: Consider using "improved" rather than "perfected," as there are still many remaining challenges associated with using the PAM-OFR.

   Response: Corrected

4. Lines 113-116: Please revise this text to make the statement a complete sentence.

   Response: The revised sentences are as follows (Lines 118-122).

   The objectives of this study are to: 1) evaluate similarities and differences among the peat source profiles from four biomes; 2) examine the extent of gas-to-particle oxidation and volatilization between 2- and 7-days of simulated atmospheric aging; and 3) characterize carbon and nitrogen properties in peat combustion emissions.

5. Line 289: Change the double-dash to a comma.

   Response: Corrected (now Lines 330-332):

Large fractions of pyrolized carbon (OP of 7–13 %) are also found, indicative of higher molecular-weight compounds that are likely to char (Chow et al., 2001; Chow et al., 2004; Chow et al., 2018).

6. Table 1: Since this table is so long, I would suggest carrying the table column labels across to each page to improve table readability.

   Response: Table 1 has been revised to show column labels on each page

7. Figure 6: I would suggest changing the y-axis range to ~70-100 so differences in less-abundant species at the top of the bars are easier to distinguish.

   Response: Figure 6 is revised with y-axis of 70–100 % to highlight changes in less abundant species.

8. Figure S1: The high-oxidation condition is given in the caption as 6.79 rather than 7 (as it is discussed in the manuscript) and should be changed.

   Response: Corrected

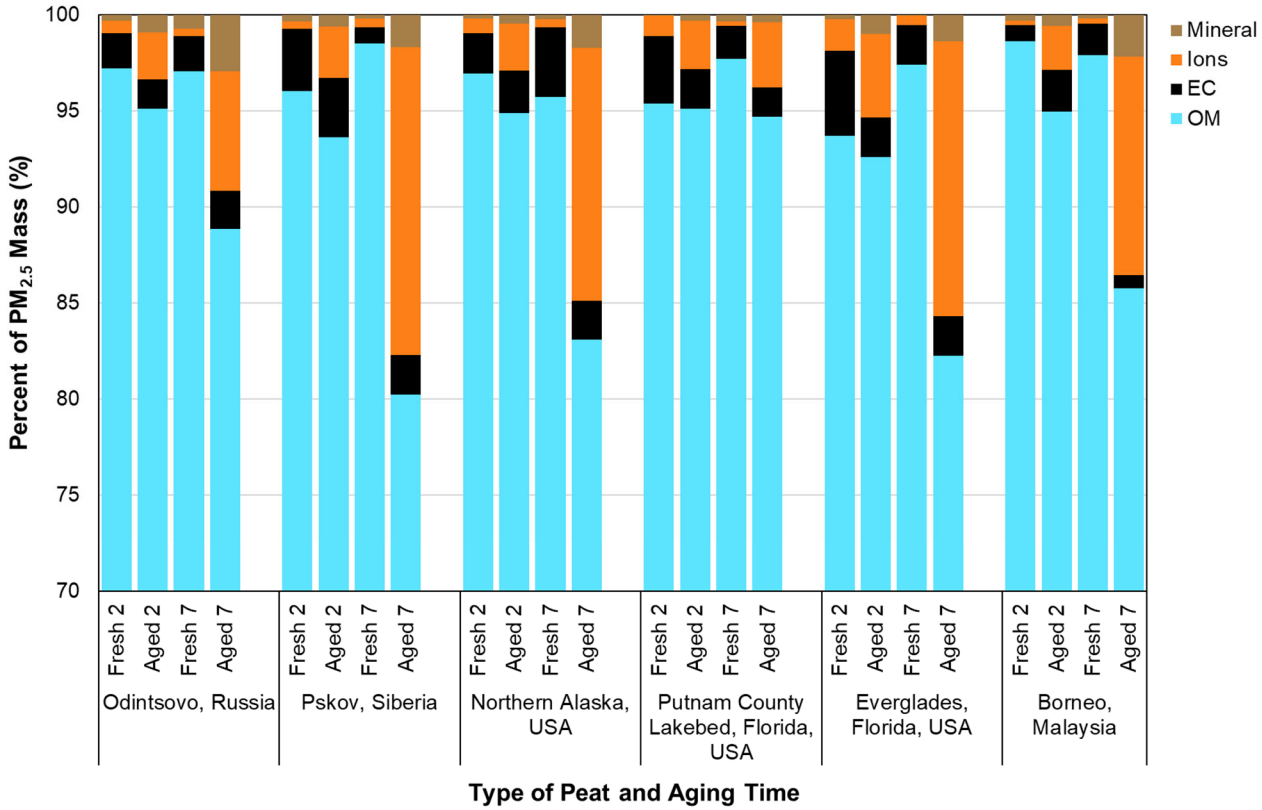

Figure 6. Reconstruction of $PM_{2.5}$ mass with organic matter (OM, see Table 3 for OM/OC ratios), elemental carbon (EC), major ions (i.e., sum of NH_4^+, NO_3^-, and $SO_4^=$), and mineral component (=2.2 Al + 2.49 Si + 1.63 Ca + 1.94 Ti + 2.42 Fe) for six types of peat between fresh and aged profiles.

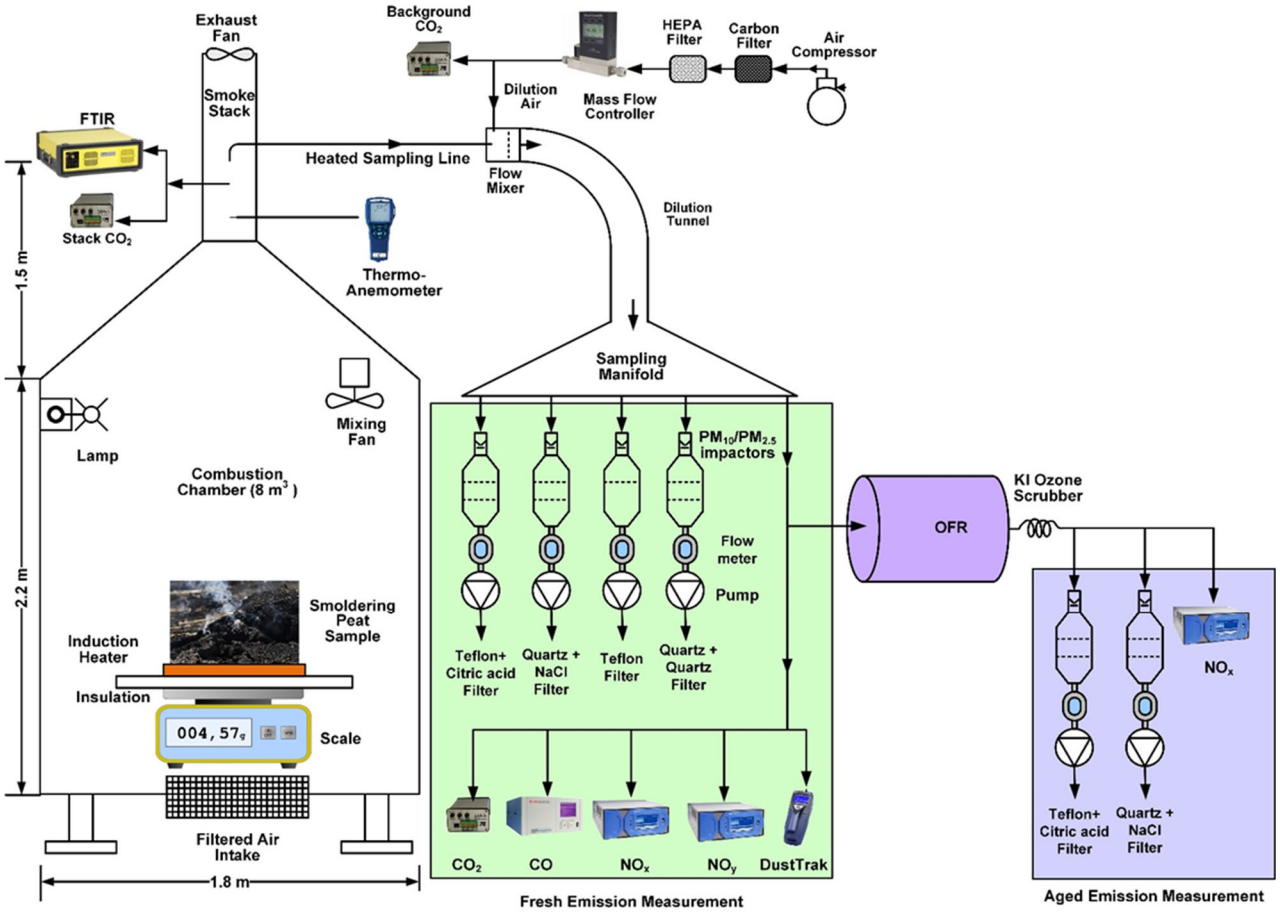

Figure S1. Configuration of peat combustion experimental set up. (FTIR: Fourier-transform infrared spectrometer; OFR: oxidation flow reactor; OFR lamps were operated at 2 and 3.5 volts to simulate aging of ~2 and 7 days, respectively) (Watson et al., 2019).

Table S1. Operational parameters for the 40 peat combustion tests

Peat Type	Peat ID	Voltage[a] (V)	Aging Time (days)	Reactor Relative Humidity (%)	Dilution Ratio	Modified Combustion Efficiency (MCE)	Peat Dry Mass before Burn (g)	Peat Dry Mass after Burn (g)	Sampling Duration (minutes)	Fresh Loading µg per filter	Aged Loading µg per filter	Ratio Aged/Fresh ± Std Dev	Fresh[b] $PM_{2.5}$ Mass µg m^{-3}	Aged[b] $PM_{2.5}$ Mass µg m^{-3}
Odintsovo, Russia	PEAT030	2	2	35	3.13	0.76	16.0	1.0	44	361.00	319.00	0.88 ± 0.019	1640.91	1450.00
	PEAT031	2	2	35	3.22	0.81	15.4	1.0	40	388.00	304.00	0.78 ± 0.017	1940.00	1520.00
	PEAT032	2	2	35	3.22	0.84	15.1	1.0	39	415.00	444.00	1.07 ± 0.018	2128.21	2276.92
	PEAT033	3.5	7	30	3.33	0.82	15.1	0.9	45	361.00	427.00	1.18 ± 0.022	1604.44	1897.78
	PEAT034	3.5	7	26	2.94	0.79	15.7	0.7	41	464.00	417.00	0.90 ± 0.015	2263.41	2034.15
	PEAT035	3.5	7	30	2.95	0.84	15.2	0.8	40	319.00	286.00	0.90 ± 0.022	1595.00	1430.00
Pskov, Siberia	PEAT023	2	2	20	5.03	0.84	47.1	1.9	67	558.00	557.00	1.00 ± 0.031	1665.67	1662.69
	PEAT025	2	2	55	4.71	0.85	25.8	1.0	70	NA[d]	257.00	NA[d]	NA[d]	734.29
	PEAT026	2	2	40	4.68	0.84	26.5	1.0	61	302.00	187.00	0.62 ± 0.0062	990.16	613.11
	PEAT027	3.5	7	40	4.68	0.87	25.6	1.0	52	206.00	142.00	0.69 ± 0.031	792.31	546.15
	PEAT028	3.5	7	50	4.72	0.83	25.7	1.1	57	384.00	411.00	1.07 ± 0.019	1347.37	1442.11
	PEAT029	3.5	7	35	4.74	0.85	26.1	1.1	68	256.00	304.00	1.19 ± 0.032	752.94	894.12
Northern Alaska, USA	PEAT013	2	2	30	4.78	0.84	58.2	13.2	95	246.00	NA[d]	NA[d]	517.89	NA[d]
	PEAT014	2	2	22	2.88	0.84	34.0	5.1	45	476.00	429.00	0.90 ± 0.014	2115.56	1906.67
	PEAT019	2	2	30	2.70	0.82	42.2	6.8	72	628.00	659.00	1.05 ± 0.012	1744.44	1830.56
	PEAT020	3.5	7	30	2.69	0.85	39.6	12.2	52	437.00	410.00	0.94 ± 0.016	1680.77	1576.92
	PEAT021[c]	3.5	7	28	2.78	0.87	40.7	13.4	48	366.00	NA[d]	NA[d]	1525.00	NA[d]
	PEAT022	3.5	7	22	2.77	0.87	38.1	14.4	48	187.00	300.00	1.60 ± 0.053	779.17	1250.00
Putnam County Lakebed, Florida, USA	PEAT007[c]	2	2	40	5.02	0.57	41.7	2.5	84	NA[d]	NA[d]	NA[d]	NA[d]	NA[d]
	PEAT008	2	2	25	5.02	0.65	40.4	1.8	73	706.00	668.00	0.95 ± 0.010	1934.25	1830.14
	PEAT009	2	2	27	5.27	0.68	40.3	2.9	68	440.00	404.00	0.92 ± 0.017	1294.12	1188.24
	PEAT042[e]	2	2	36	5.04	0.72	37.5	1.9	65	382.00	357.00	0.93 ± 0.019	1175.38	1098.46
	PEAT043[e]	2	2	22	5.01	0.71	37.0	1.9	68	381.00	363.00	0.95 ± 0.019	1120.59	1067.65
	PEAT044[e]	2	2	22	4.98	0.73	38.3	2.0	69	356.00	363.00	1.02 ± 0.021	1031.88	1052.17
	PEAT004[c]	3.5	7	40	4.89	0.63	39.6	1.9	81	NA[d]	594.00	NA[d]	NA[d]	1466.67
	PEAT005	3.5	7	43	4.89	0.67	37.5	2.0	88	713.00	847.00	1.19 ± 0.011	1620.45	1925.00
	PEAT006	3.5	7	44	4.90	0.58	38.3	2.5	91	648.00	657.00	1.01 ± 0.011	1424.18	1443.96
Everglades National Park, Florida, USA	PEAT010	2	2	25	5.13	0.91	41.3	13.9	111	182.00	340.00	1.87 ± 0.062	327.93	612.61
	PEAT011	2	2	25	4.10	0.90	61.2	21.5	135	545.00	487.00	0.89 ± 0.012	807.41	721.48
	PEAT012	2	2	17	4.09	0.95	66.5	29.1	119	262.00	247.00	0.94 ± 0.027	440.34	415.13
	PEAT015	2	2	30	3.97	0.87	31.8	11.0	55	227.00	223.00	0.98 ± 0.032	825.45	810.91
	PEAT016	3.5	7	33	4.21	0.90	64.7	31.1	85	232.00	410.00	1.77 ± 0.046	545.88	964.71
	PEAT017	3.5	7	48	4.03	0.88	64.2	16.1	113	496.00	971.00	1.96 ± 0.024	877.88	1718.58
	PEAT018	3.5	7	40	4.04	0.89	61.8	35.2	57	225.00	369.00	1.64 ± 0.044	789.47	1294.74
Borneo, Malaysia	PEAT036	2	2	37	2.97	0.87	30.3	9.3	66	406.00	322.00	0.79 ± 0.017	1230.30	975.76
	PEAT037[c]	2	2	42	2.98	0.82	29.9	7.0	69	368.00	NA[d]	NA[d]	1066.67	NA[d]
	PEAT038	2	2	43	3.02	0.83	30.4	4.2	65	508.00	459.00	0.90 ± 0.014	1563.08	1412.31
	PEAT039	3.5	7	42	3.03	0.82	29.4	7.6	61	343.00	406.00	1.18 ± 0.024	1124.59	1331.15
	PEAT040[c]	3.5	7	38	3.00	0.81	31.0	4.1	66	458.00	NA[d]	NA[d]	1387.88	NA[d]
	PEAT041	3.5	7	38	3.02	0.81	31.5	7.0	71	419.00	459.00	1.10 ± 0.019	1180.28	1292.96

[a]Ultraviolet lamp voltages (OFR185 mode) were used to simulate 2- and 7-days of atmospheric aging

[b]Based on 5 L min^{-1} flow rate
[c]These unpaired samples (fresh and aged, n=5) are not included in the averages by peat type
[d]Data not available
[e]Samples are with 60 % fuel moisture (n=3) and are treated separately from others (25 % fuel moisture)

Table A. OFR source testing examples and PM enhancement after oxidation (Cao et al., 2019)

Source/Reference	PM Enhancement[a]	Location and Time	Comments[b]
Multiple vehicle engine exhaust (Tkacik et al., 2014)	• PM increased 5 (0.5 day aging) to 10 (2-day aging) times on average, mostly due to SOA and NH_3NO_3. • NH_4NO_3 increased twice as much as SOA.	• Fort Pitt Tunnel, Pittsburgh, PA, May 2013	• 90-96% light duty gasoline vehicles. • .03-9.3 days equivalent aging, assuming $3x10^6$ molecules/cm^3 average daily OH. • AACSM measured major PM components
Gasoline Direct Injection Engine Exhaust (Karjalainen et al., 2016)	• PM increased by factor of ~22 for cold start, factor of 8 for highway driving, and factor of ~4 for highway cruising, mostly due to SOA.	• Laboratory roller dynamometer with New European Driving Cycle (NEDC)	• Stainless steel 13 L OFR185 • 2011 turbocharged 1.4L turbo-charged engine in passenger car • 10% ethanol in low sulfur gasoline fuel (<10 ppmwS) • ~8 days equivalent aging assuming $1.5x10^6$ molecules/cm^3 ambient average OH • AMS measured major PM components
Diesel engine exhaust (Jathar et al., 2017)	• SOA was 12 to 25 times POA without after treatments, 80-800 time POA with after treatments.	• Laboratory engine dynamometer. Diesel and biodiesel fuels, with and without after treatment	• Aerodyne OFR185 • 0.4 to 2 days equivalent aging assuming $1.5x10^6$ molecules/cm^3 ambient average OH • 4.5 L Deer4045 Powertech engine with oxidation catalyst and particulate filter • Output sampled by AMS, SMPS, PAX
Heated cooking oil (Liu et al., 2017a)	• Average SOA production of 1.35±0.3 µg/min.	• Laboratory, heated various oils to 240°C	• OFR254-40 irradiation • ~1.3 days aging assuming $1.5x10^6$ molecules/cm^3 ambient average OH • AMS measured major PM components • Filtered out primary particles prior to OFR

		for 2 min.	
Wood, peat, shrub, and grass burning (Ortega et al., 2013)	• Organic aerosol mass changed from 0.8 for ponderosa pine to 2.1 times POA for sage	• Laboratory burn chamber	• OFR185 irradiation • ~0.1 to ~5 days assuming $1.5x10^6$ molecules/cm^3 ambient average OH • Fuels included ponderosa pine, lodgepole pine, peat, Alaskan duff, gallberry, black spruce, pocosin, turkey oak, saw grass, wire grass, ceanothus, manzanita, white spruce, wheat straw, chamise, and sage. • AMS measured major components.
Peat and biomass burning (Bhattarai et al., 2018)	• Particle numbers increased by 2.2 to 28 for the different fuels. • OC mass decreased by 9% to 13% for peat emissions, 7% for fir/aspen emissions, and 0% for shrub emissions.	• Laboratory combustion chamber (Tian et al., 2015)	• Aerodyne OFR185 • Siberian, Florida, and Malaysian peats. High desert shrubs, Douglas fir, and aspen. • Output sampled onto Teflon and Teflon-coated glass fiber filters with XAD backup for laboratory analyses. SMPS measured particle number and PAX measured particle absorption. • 7-day equivalent aging assuming $1.56x10^6$ molecules/cm^3 ambient average OH
Oak leaf and heartwood burning (Fortenberry et al., 2018)	• Leaf PM organic concentrations changed by 1.6 and 1.06 times after 1-3 and 6-10 days aging. • Heartwood PM organic concentrations changed by 0.72 and 0.84 times after 1-3 and 6-10 days aging.	• Laboratory combustion chamber	• Aerodyne OFR 185 • 0, 1-3, and 6-10 day equivalent aging assuming $1.5x10^6$ molecules/cm^3 ambient average OH • Output sampled by AMS, SMPS, and TAG for PM characterization
Solid fuel cook stoves (Reece et al., 2017)	• TSF organic aerosol increased 2.5 times POA after 4 days and 2 times after 14 days • RS organic aerosol increased 2 times	• Laboratory combustion chamber. Water boiling	• Custom built 7L OFR (Table 1) • Three stone fire (TSF), rocket stove (RS), and forced-draft gasifier fan stove (FDGS) were tested with dry red oak wood fuel • AACSM, PSX, SMPS, and filter samples for PM characterization • 2 to 14 days aging, assuming $1.5x10^6$ molecules/cm^3

	POA after 3 days and 1.5 times after 12 days. • FDGS increased 1.2 times after 3 and 11 days.	test and cold start/simmering cycles	

[a]POA=Primary organic aerosol, SOA=Secondary Organic Aerosol.
[b]Particle measurement instruments: AMS=Aerodyne Mass Spectrometer (various types), AACSM=Aerodyne Aerosol Chemical Speciation Monitor, TAG=Thermal desorption Aerosol Gas chromatograph, SMPS=Scanning Mobility Particle Sizer, PAX=Photoacoustic extinctiometer.

References

Aerodyne: PAM users manual, Aerodyne Research Inc., Billerica, MA, 2019a. https://pamusersmanual.jimdo.com/

Aerodyne: Potential Aerosol Mass (PAM) oxidation flow reactor, Aerodyne Research Inc., Billerica, MA, 2019b. http://www.aerodyne.com/sites/default/files/u17/PAM%20Potential%20Aerosol%20Mass%20Reactor.pdf

Altshuller, A. P.: Ambient air hydroxyl radical concentrations: Measurements and model predictions, J. Air Pollut. Control Assoc., 39, 704-708, 1989.

Bhattarai, C., Samburova, V., Sengupta, D., Iaukea-Lum, M., Watts, A. C., Moosmuller, H., and Khlystov, A. Y.: Physical and chemical characterization of aerosol in fresh and aged emissions from open combustion of biomass fuels, Aerosol Sci. Technol., 52, 1266-1282, 2018.

BHK: Products: Mercury lamps, BHK Inc., Ontario, CA, 2019. http://www.bhkinc.com/index.cfm?action=products

Bin Babar, Z., Park, J. H., and Lim, H. J.: Influence of NH3 on secondary organic aerosols from the ozonolysis and photooxidation of alpha-pinene in a flow reactor, Atmos. Environ., 164, 71-84, 2017.

Budisulistiorini, S. H., Riva, M., Williams, M., Miyakawa, T., Chen, J., Itoh, M., Surratt, J. D., and Kuwata, M.: Dominant contribution of oxygenated organic aerosol to haze particles from real-time observation in Singapore during an Indonesian wildfire event in 2015, Atmos. Chem. Phys, 18, 16481-16498, 2018.

Cao, J. J.: A brief introduction and progress summary of the $PM_{2.5}$ source profile compilation project in China, Aerosol Science and Engineering, 2, 43-50, 2018.

Cao, J. J., Wang, Q. Y., Tan, J., Zhang, Y. G., Wang, W. J., Zhong, B. L., Ho, S. S. H., Chen, L.-W. A., Wang, X. L., Watson, J. G., and Chow, J. C.: Evaluation of the oxidation flow reactor for particulate matter emission limit certification, Atmos. Environ., 2019. submitted, 2019.

CARB: Speciation profiles used in ARB modeling, California Air Resources Board, Sacramento, CA, 2019. http://arb.ca.gov/ei/speciate/speciate.htm

Cazorla, M. and Brune, W. H.: Measurement of ozone production sensor, Atmos. Meas. Tech., 3, 545-555, 2010.

Chow, J. C., Engelbrecht, J. P., Watson, J. G., Wilson, W. E., Frank, N. H., and Zhu, T.: Designing monitoring networks to represent outdoor human exposure, Chemosphere, 49, 961-978, 2002.

Chow, J. C., Riggio, G. M., Wang, X. L., Chen, L.-W. A., and Watson, J. G.: Measuring the organic carbon to organic matter multiplier with thermal/optical carbon mass spectrometer analyses, Aerosol Science and Engineering, 2, 165-172, 2018.

Chow, J. C., Watson, J. G., Chen, L.-W. A., Arnott, W. P., Moosmüller, H., and Fung, K. K.: Equivalence of elemental carbon by Thermal/Optical Reflectance and Transmittance with different temperature protocols, Environ. Sci. Technol., 38, 4414-4422, 2004.

Chow, J. C., Watson, J. G., Crow, D., Lowenthal, D. H., and Merrifield, T. M.: Comparison of IMPROVE and NIOSH carbon measurements, Aerosol Sci. Technol., 34, 23-34, 2001.

Dall'Osto, M., Ovadnevaite, J., Ceburnis, D., Martin, D., Healy, R. M., O'Connor, I. P., Kourtchev, I., Sodeau, J. R., Wenger, J. C., and O'Dowd, C.: Characterization of urban aerosol in Cork city (Ireland) using aerosol mass spectrometry, Atmos. Chem. Phys, 13, 4997-5015, 2013.

Davis, D. D., Ravishankara, A. R., and Fischer, S.: SO_2 oxidation via the hydroxyl radical-Atmospheric fate of HSO_x radicals, Geophysical Research Letters, 6, 113-116, 1979.

Ezell, M. J., Johnson, S. N., Yu, Y., Perraud, V., Bruns, E. A., Alexander, M. L., Zelenyuk, A., Dabdub, D., and Finlayson-Pitts, B. J.: A new aerosol flow system for photochemical and thermal studies of tropospheric aerosols, Aerosol Sci. Technol., 44, 329-338, 2010.

Fortenberry, C. F., Walker, M. J., Zhang, Y. P., Mitroo, D., Brune, W. H., and Williams, B. J.: Bulk and molecular-level characterization of laboratory-aged biomass burning organic aerosol from oak leaf and heartwood fuels, Atmos. Chem. Phys, 18, 2199-2224, 2018.

Fujii, Y., Tohno, S., Amil, N., and Latif, M. T.: Quantitative assessment of source contributions to $PM_{2.5}$ on the west coast of Peninsular Malaysia to determine the burden of Indonesian peatland fire, Atmos. Environ., 171, 111-117, 2017.

Hidy, G. M.: Atmospheric chemistry in a box or a bag, Atmosphere, 10, 1-36, 2019.

Huang, Y., Coggon, M. M., Zhao, R., Lignell, H., Bauer, M. U., Flagan, R. C., and Seinfeld, J. H.: The Caltech Photooxidation Flow Tube reactor: Design, fluid dynamics and characterization, Atmos. Meas. Tech., 10, 839-867, 2017.

Jathar, S. H., Friedman, B., Galang, A. A., Link, M. F., Brophy, P., Volckens, J., Eluri, S., and Farmer, D. K.: Linking load, fuel, and emission controls to photochemical production of secondary organic aerosol from a diesel engine, Environ. Sci. Technol., 51, 1377-1386, 2017.

Jimenez, J. L.: Oxidation flow reactors (including PAM): Principles and best practices for applications in aerosol research, 2018 International Aerosol Conference Tutorial, St. Louis, MO, 2018. https://docs.google.com/viewer?a=v&pid=sites&srcid=ZGVmYXVsdGRvbWFpbnxwYW13aWtpfGd4OjY0N2MyYTZkYThiODU0MTM
Kang, E., Root, M. J., Toohey, D. W., and Brune, W. H.: Introducing the concept of Potential Aerosol Mass (PAM), Atmos. Chem. Phys, 7, 5727-5744, 2007.
Karjalainen, P., Timonen, H., Saukko, E., Kuuluvainen, H., Saarikoski, S., Aakko-Saksa, P., Murtonen, T., Bloss, M., Dal Maso, M., Simonen, P., Ahlberg, E., Svenningsson, B., Brune, W. H., Hillamo, R., Keskinen, J., and Ronkko, T.: Time-resolved characterization of primary particle emissions and secondary particle formation from a modern gasoline passenger car, Atmos. Chem. Phys, 16, 8559-8570, 2016.
Keller, A. and Burtscher, H.: A continuous photo-oxidation flow reactor for a defined measurement of the SOA formation potential of wood burning emissions, J. Aerosol Sci., 49, 9-20, 2012.
Kourtchev, I., Hellebust, S., Bell, J. M., O'Connor, I. P., Healy, R. M., Allanic, A., Healy, D., Wenger, J. C., and Sodeau, J. R.: The use of polar organic compounds to estimate the contribution of domestic solid fuel combustion and biogenic sources to ambient levels of organic carbon and PM2.5 in Cork Harbour, Ireland, Sci. Total Environ, 409, 2143-2155, 2011.
Lambe, A. T., Ahern, A. T., Williams, L. R., Slowik, J. G., Wong, J. P. S., Abbatt, J. P. D., Brune, W. H., Ng, N. L., Wright, J. P., Croasdale, D. R., Worsnop, D. R., Davidovits, P., and Onasch, T. B.: Characterization of aerosol photooxidation flow reactors: heterogeneous oxidation, secondary organic aerosol formation and cloud condensation nuclei activity measurements, Atmos. Meas. Tech., 4, 445-461, 2011.
Lee, S. B., Bae, G. N., and Moon, K. C.: Smog chamber measurements. In: Atmosheric and Biological Environmental Monitoring, Kim, Y. J., Platt, U., Gu, M. B., and Iwahashi, H. (Eds.), Springer, Dordrecht, Netherlands, 2009.
Li, R., Palm, B. B., Ortega, A. M., Hlywiak, J., Hu, W. W., Peng, Z., Day, D. A., Knote, C., Brune, W. H., de Gouw, J. A., and Jimenez, J. L.: Modeling the radical chemistry in an oxidation flow reactor: Radical formation and recycling, sensitivities, and the OH exposure estimation equation, Journal of Physical Chemistry A, 119, 4418-4432, 2015.
Lin, C. S., Ceburnis, D., Huang, R. J., Canonaco, F., Prevot, A. S. H., O'Dowd, C., and Ovadnevaite, J.: Summertime aerosol over the west of Ireland dominated by secondary aerosol during long-range transport, Atmosphere, 10, 2019.
Liu, T. Y., Li, Z. J., Chan, M. N., and Chan, C. K.: Formation of secondary organic aerosols from gas-phase emissions of heated cooking oils, Atmos. Chem. Phys, 17, 7333-7344, 2017a.
Liu, Y. Y., Zhang, W. J., Bai, Z. P., Yang, W., Zhao, X. Y., Han, B., and Wang, X. H.: China Source Profile Shared Service (CSPSS): The Chinese $PM_{2.5}$ database for source profiles, Aerosol Air Qual. Res., 17, 1501-1514, 2017b.
Mao, J., Ren, X., Brune, W. H., Olson, J. R., Crawford, J. H., Fried, A., Huey, L. G., Cohen, R. C., Heikes, B., Singh, H. B., Blake, D. R., Sachse, G. W., Diskin, G. S., Hall, S. R., and Shetter, R. E.: Airborne measurement of OH reactivity during INTEX-B, Atmos. Chem. Phys, 9, 163-173, 2009.
Mitroo, D., Sun, Y. J., Combest, D. P., Kumar, P., and Williams, B. J.: Assessing the degree of plug flow in oxidation flow reactors (OFRs): a study on a potential aerosol mass (PAM) reactor, Atmos. Meas. Tech., 11, 1741-1756, 2018.
Mo, Z. W., Shao, M., and Lu, S. H.: Compilation of a source profile database for hydrocarbon and OVOC emissions in China, Atmos. Environ., 143, 209-217, 2016.
Ortega, A. M., Day, D. A., Cubison, M. J., Brune, W. H., Bon, D., de Gouw, J. A., and Jimenez, J. L.: Secondary organic aerosol formation and primary organic aerosol oxidation from biomass-burning smoke in a flow reactor during FLAME-3, Atmos. Chem. Phys, 13, 11551-11571, 2013.
PAMWiki: PAMWiki, 2019. https://sites.google.com/site/pamwiki/
Peng, Z., Day, D. A., Ortega, A. M., Palm, B. B., Hu, W. W., Stark, H., Li, R., Tsigaridis, K., Brune, W. H., and Jimenez, J. L.: Non-OH chemistry in oxidation flow reactors for the study of atmospheric chemistry systematically examined by modeling, Atmos. Chem. Phys, 16, 4283-4305, 2016.
Peng, Z., Day, D. A., Stark, H., Li, R., Lee-Taylor, J., Palm, B. B., Brune, W. H., and Jimenez, J. L.: HO_x radical chemistry in oxidation flow reactors with low-pressure mercury lamps systematically examined by modeling, Atmos. Meas. Tech., 8, 4863-4890, 2015.
Peng, Z. and Jimenez, J. L.: Modeling of the chemistry in oxidation flow reactors with high initial NO, Atmos. Chem. Phys., 17, 11991-12010, 2017.

Peng, Z., Palm, B. B., Day, D. A., Talukdar, R. K., Hu, W. W., Lambe, A. T., Brune, W. H., and Jimenez, J. L.: Model evaluation of new techniques for maintaining high-NO conditions in oxidation flow reactors for the study of OH-initiated atmospheric chemistry, Acs Earth and Space Chemistry, 2, 72-86, 2018.
Pernigotti, D., Belis, C. A., and Spanò, L.: SPECIEUROPE: The European data base for PM source profiles, Atmospheric Pollution Research, 7, 307-314, 2016.
Pourkhesalian, A. M., Stevanovic, S., Rahman, M. M., Faghihi, E. M., Bottle, S. E., Masri, A. R., Brown, R. J., and Ristovski, Z. D.: Effect of atmospheric aging on volatility and reactive oxygen species of biodiesel exhaust nano-particles, Atmos. Chem. Phys, 15, 9099-9108, 2015.
Pratap, V., Bian, Q. J., Kiran, S. A., Hopke, P. K., Pierce, J. R., and Nakao, S.: Investigation of levoglucosan decay in wood smoke smog-chamber experiments: The importance of aerosol loading, temperature, and vapor wall losses in interpreting results, Atmos. Environ., 199, 224-232, 2019.
Reece, S. M., Sinha, A., and Grieshop, A. P.: Primary and photochemically aged aerosol emissions from biomass cookstoves: Chemical and physical vharacterization, Environ. Sci. Technol., 51, 9379-9390, 2017.
Sander, S. P., Friedl, R. R., Ravishankara, A. R., Golden, D. M., Kolb, C. E., Kurylo, M. J., Molina, M. J., Moortgat, G. K., Finlayson-Pitts, B. J., Wine, P. H., R.E., H., and Orkin, V. L.: Chemical kinetics and photochemica data for use in atmospheric studies: Evaluatoin Number 15, Jet Propulsion Laboratory, Pasadena, CA, 2006. https://jpldataeval.jpl.nasa.gov/pdf/JPL_15_AllInOne.pdf
See, S. W., Balasubramanian, R., Rianawati, E., Karthikeyan, S., and Streets, D. G.: Characterization and source apportionment of particulate matter <= 2.5 mu m in Sumatra, Indonesia, during a recent peat fire episode, Environ. Sci. Technol., 41, 3488-3494, 2007.
Smith, J. D., Kroll, J. H., Cappa, C. D., Che, D. L., Liu, C. L., Ahmed, M., Leone, S. R., Worsnop, D. R., and Wilson, K. R.: The heterogeneous reaction of hydroxyl radicals with sub-micron squalane particles: a model system for understanding the oxidative aging of ambient aerosols, Atmos. Chem. Phys, 9, 3209-3222, 2009.
Stone, D., Whalley, L. K., and Heard, D. E.: Tropospheric OH and HO2 radicals: field measurements and model comparisons, Chemical Society Reviews, 41, 6348-6404, 2012.
Tham, J., Sarkar, S., Jia, S. G., Reid, J. S., Mishra, S., Sudiana, I. M., Swarup, S., Ong, C. N., and Yu, L. Y. E.: Impacts of peat-forest smoke on urban PM2.5 in the Maritime Continent during 2012-2015: Carbonaceous profiles and indicators, Environ. Pollut., 248, 496-505, 2019.
Tian, J., Chow, J. C., Cao, J. J., Han, Y. M., Ni, H. Y., Chen, L.-W. A., Wang, X. L., Huang, R. J., Moosmüller, H., and Watson, J. G.: A biomass combustion chamber: Design, evaluation, and a case study of wheat straw combustion emission tests, Aerosol Air Qual. Res., 15, 2104-2114, 2015.
Tkacik, D. S., Lambe, A. T., Jathar, S., Li, X., Presto, A. A., Zhao, Y. L., Blake, D., Meinardi, S., Jayne, J. T., Croteau, P. L., and Robinson, A. L.: Secondary organic aerosol formation from in-use motor vehicle emissions using a potential aerosol mass reactor, Environ. Sci. Technol., 48, 11235-11242, 2014.
U.S.EPA: SPECIATE Version 5.0, U.S. Environmental Protection Agency, Research Triangle Park, NC, 2019. https://www.epa.gov/air-emissions-modeling/speciate-version-45-through-40
Watson, J. G., Chow, J. C., Wang, X. L., Kohl, S. D., Chen, L.-W. A., and Etyemezian, V. R.: Overview of real-world emission characterization methods. In: Alberta Oil Sands: Energy, Industry, and the Environment, Percy, K. E. (Ed.), Developments in Environmental Science, Elsevier Press, Amsterdam, The Netherlands, 2012.